



Cancelling the effect of sharp notches or cracks with graded elastic modulus materials

M. Ciavarella*

Politecnico di BARI, DMMM department, Viale Gentile 182, 70126 Bari, Italy

Hamburg University of Technology, Department of Mechanical Engineering, Am Schwarzenberg-Campus 1, 21073 Hamburg, Germany

ARTICLE INFO

Keywords:

Notches
Cracks
FGM
Additive manufacturing
Graded materials
Biomimetics

ABSTRACT

Recent technologies permit to build materials which have elastic spatially varying modulus which can also imitate solutions adopted in Nature to optimize some structures. It has been shown that for example the stress concentration due to a hole in an infinite plate can be cancelled with a radially varying modulus making it similar to load-bearing bones which seem to resist structural failures even in the presence of blood vessel holes (foramina). Here, we attempt to study the classical problem of a sharp wedge (which includes the important case of a crack) looking for stresses varying as power law of the distance from the notch tip, $\sigma \sim r^\alpha$, with a modulus varying as $E \sim r^\beta$. In the inhomogeneous case the order of singularity of the LEM case decreases if $\beta > 0$, as confirmed by FEM investigations. Hence, we can remove stress singularities, which suggests an interesting alternative to the “rounding” of the notch. More in general, since for many materials it has been found that both strength and modulus are power laws of the density, using the so called strength-modulus exponent ratio we can obtain optimal design by keeping the asymptotic stress constantly equal to the strength. The present investigation paves the way for a new optimization strategy in the problems which eliminates size-scale effects due to singular stress fields, with potentially very wide applications.

1. Introduction

Functionally graded materials (FGM) exist in nature (soils, bones, etc.), but with the advent of various advanced manufacturing techniques, are emerging also in various areas of technology to engineer the resistance to stress concentrations, thermal stresses, pressure-loading, etc. Applications range from aerospace, as they withstand very high thermal gradient, medicine in dental and orthopedic applications for teeth and bone replacement, in defence for armor plates and bullet-proof vests, in energy conversion devices and as protective coating on turbine blades in gas turbine engine (Li and Han, 2018). In some cases, the use of controlled gradients in elastic properties has been clearly demonstrated also experimentally to improve resistance due to the reduction in stress concentration, as in the case of sliding-contact damage (Suresh et al., 1999).

Depending on the application, the microstructure can be allowed to vary along one or several directions. Structures with spatially varying elastic modulus emerge also from the very popular relatively recent technique of topological optimization (Bendsøe and Sigmund, 1999). In particular the “black and white” optimization (which may result in easier products to manufacture) is numerically more challenging than the “grey” optimization where the modulus is varying in a continuous scale by using a density parameter.

* Correspondence to: Politecnico di BARI, DMMM department, Viale Gentile 182, 70126 Bari, Italy.

E-mail address: Mciava@poliba.it.

For many materials including cellular materials (Gibson and Ashby, 1997) or bones (Martin, 1991), the Young's modulus E varies as power law of the density ρ

$$E = P\rho^p \quad (1)$$

with P, p being material properties. There are so called Hashin–Shtrikman bounds for two-phase materials on the value of p ($p \geq 3$ in plane elasticity, for example, see Bendsøe and Sigmund 1999), but for example in bones, Young's modulus is found to vary approximately with the cubic power of the density (and also of mineral content) (Currey, 1988). For 3D cellular materials, the elastic modulus tends to scale as the square of the relative density (Gibson, 1989). Graded materials have been manufactured by a variety of processes including centrifugal molding, pressureless sintering, suspension of particles in polymer matrix, spark plasma sintering or laser melt injection (see a recent review Kumar et al., 2023). Zhang et al. (2018) review the development of the additive manufacturing techniques on FGM. In advanced printing techniques involving complex geometries at nanoscale, such as two-photon polymerization direct laser writing (TPP-DLW), the obtained polymer mechanical properties depend on applied process parameters (Bauer et al., 2019) so in principle FGM could be developed even down to nanoscale. Schumacher et al. (2015) have demonstrated the possibility to create FGM in the area of metamaterials, with microstructures different for each cell and not only their density.

One of the cases studied in the literature is that of the classical Kirsch problem of the Stress Concentration Factor around a circular hole in an infinite plate subjected to uniform tension with for graded material has been studied by several authors (Huang et al., 2003; Kubair and Bhanu-Chandar, 2008; Kumar et al., 2023; Mohammadi et al., 2011; Shi, 2015; Abdalla et al., 2023), also inspired by load-bearing bones for which the presence of blood vessel holes (foramina) seem to have no effect on resistance. Götzen et al. (2003) suggested that in a horse metacarpal bone there is a compliant region near the foramen and a stiffer region at some distance away, with respect to far field normal bone properties. Huang et al. (2003) studied in detail the optimization of a plate with a hole in considering that not only the elastic modulus is related to the apparent density ρ by a power law functions similar to Eq. (1), but also limit or “allowable” strength σ_{allow}

$$\sigma_{allow} = Q\rho^\delta \quad (2)$$

so that if we eliminate the density from Eqs. (1) and (2), we obtain

$$\sigma_{allow} = CE^{\delta/p} \quad (3)$$

where C, P, Q, δ, p, q are material constants, in some cases provided by models for cellular materials (Gibson and Ashby, 1997) or bones (Martin, 1991).

The ratio δ/p is called *strength-modulus exponent ratio* and classifies materials since when $\delta/p < 1$ strength increases slower than elastic modulus when the density is increased (the shaded area in Fig. 1). Only when $\delta/p = 0$, structural optimization is *identical* to stress concentration minimization (the lower horizontal line in Fig. 1). Judging from the very wide Ashby charts in (Ashby, 1991), it is clear that elastic modulus has 5 decades change over a little more than 2 decades change of density, while strength has about 4 decades change, and in general elastic modulus varies more wildly than strength. Hence, it is likely that for most materials $\delta/p < 1$ would be the correct range (which is why we indicated it as “more common range” in Fig. 1, which includes the stress concentration criterion as a subcase).

Huang et al. (2003) demonstrated for the case of a plate with a circular hole that the effect of the hole was eliminated by locally stiffening areas that experience high stresses when $\delta/p > 1$ and the opposite for $\delta/p < 1$ like in the case of the bone where reducing the modulus near the hole boundary and increasing it some distance away was optimal, as found by Götzen et al. (2003) in real bones. In other words, real bones seem to suggest an optimization criterion similar to stress reduction. Also the attachment of tendon to bone seems to have an optimal design whereby the “insertion site” has a compliant interfacial zone, not regenerated following healing. Indeed, it has been shown that the stress concentrations is reduced by a biomimetic grading of material properties (Liu et al., 2012).

Also in singular stress field cases problems have been solved. For example, Kossa et al. (2023) have studied the case of a cylindrical elastic punch attached to a rigid halfspace with a radially varying modulus, and used a linearly varying elastic modulus which remains finite both at the centre and at the outer edge of the punch, leaving the order of the singular stress unchanged and unaffected by grading. Therefore, their optimization of the elastic modulus finds that for softer edges than the core of the punch, the adhesion strength is increased — assuming the critical energy release rate is unaffected by the elastic modulus.

Here, we consider the very classical problem of an elastic sharp wedge $-\gamma < \theta < \gamma$ (see Fig. 2) studied by Williams in the homogeneous case (see Barber, 2002) which for $\gamma = \pi$ becomes the case of a crack. This problem is so far completely neglected for the graded material case, in the best of the author's knowledge, despite for the homogeneous sharp V notch the Literature is very vast, witnessing the importance of this problem in static and fatigue assessment of structures (Carpinteri et al., 2008; Gómez and Elices, 2003; Lazzarin and Zambardi, 2001; Meneghetti and Lazzarin, 2007; Lazzarin et al., 2014; Seweryn, 1994). The only exception is Carpinteri and Paggi (2005) which however consider angular grading which does not significantly alter the order of singularity in the stress field: more specifically it is possible to analytically demonstrate that the stress-field is nonsingular only in a degenerate case where the entire region is with zero elastic modulus.

Obviously the case of sharp crack is even more of importance because we can study propagation which becomes self-similar and not only initiation (Broek, 2012; Gdoutos, 2020), and the crack case has a history of more than one hundred years since Griffith (1921).¹ However, since cracks appear naturally in structures, it may be more difficult to “optimize” the elastic modulus in the

¹ Probably one of the most cited papers in mechanics of materials with over 20000 citations in Google Scholar.

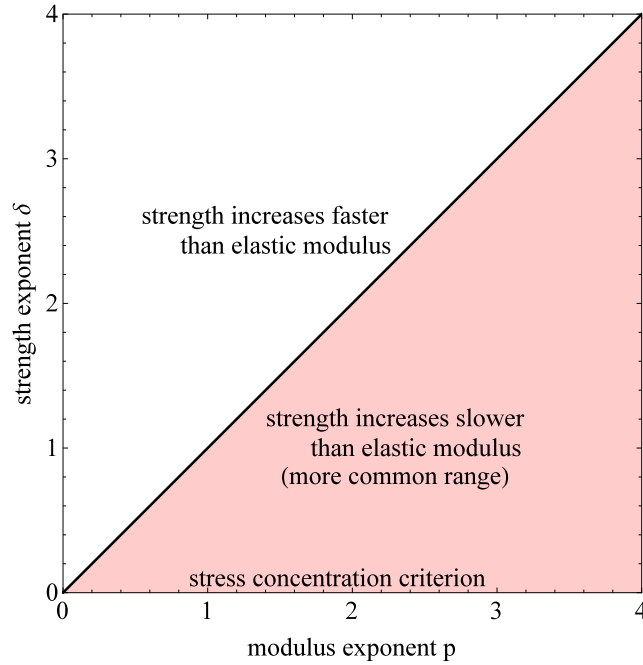


Fig. 1. The plane p, δ where p is the power law exponent of elastic modulus and δ the strength exponent. Their ratio δ/p is called *strength-modulus exponent ratio*.

proximity of the crack tip, which would be unknown in advance, unless we can take active action at the crack tip. This is the case considered by Liu et al. (2023) who apply light at the crack tip of a sample of special materials, or in the emerging area of self-healing materials (Song et al., 2021).

In all these classical studies, concepts are derived to deal with the stress singularity: for the crack case, the well known Griffith theory associates to the classical singular field an energy release rate G with crack advancement, as per the Irwin equation $G = K_I^2/E$ where K_I is the multiplier of the stress field of dimensions $\text{stress} \times \text{length}^{0.5}$. For a sharp notch, one can generalize the concept by assuming that failure occurs when the generalized multiplier K_I^V of the stress field of dimensions $\text{stress} \times \text{length}^{-\alpha}$ reaches a critical value, or else one can imagine a small crack immersed in the notch singular field, and compute the associated stress intensity factor K_I of standard meaning. In the case of homogeneous material, it is rather expected that reducing the singularity, leads to an improvement of strength, but more precisely to compare two conditions both the order of singularity and the strength of the singular field must be considered. For the inhomogeneous material, the matter is even more complex and certainly there is very little experimental investigation in the Literature, although we shall give some suggestions in the Discussion paragraph about what could seem to be an optimality condition.

As for a crack, the loading in a notch can activate symmetrical or antisymmetric responses, which for in plane loading such as that studied here, are called mode I and mode II loading (see Fig. 2). In particular, it is known that the mode I singularity for the homogeneous material is dominant with respect to the mode II one, except in the limit case of the crack, when they coincide.

2. Solution for the notch with power law modulus

Consider a semi-infinite notch defined by $0 \leq r \leq \infty$, and an Airy stress function $\varphi(r, \theta)$ which defines stresses as

$$\sigma_{rr}(r, \theta) = \frac{1}{r} \frac{\partial \varphi(r, \theta)}{\partial r} + \frac{1}{r^2} \frac{\partial^2 \varphi(r, \theta)}{\partial \theta^2} \tag{4}$$

$$\sigma_{\theta\theta}(r, \theta) = \frac{\partial^2 \varphi(r, \theta)}{\partial r^2} \tag{5}$$

$$\sigma_{r\theta}(r, \theta) = -\frac{\partial}{\partial r} \left(\frac{1}{r} \frac{\partial \varphi(r, \theta)}{\partial \theta} \right) \tag{6}$$

where due to geometry, and assuming tractions vary as $\sigma \sim r^\alpha$, we can take in the form of separated variables as in classical case (see Barber, 2002, 11.1)

$$\varphi(r, \theta) = r^{\alpha+2} f(\theta) \tag{7}$$

Hence stresses are

$$\sigma_{rr}(r, \theta) = r^\alpha [(\alpha + 2) f(\theta) + f''(\theta)] \tag{8}$$

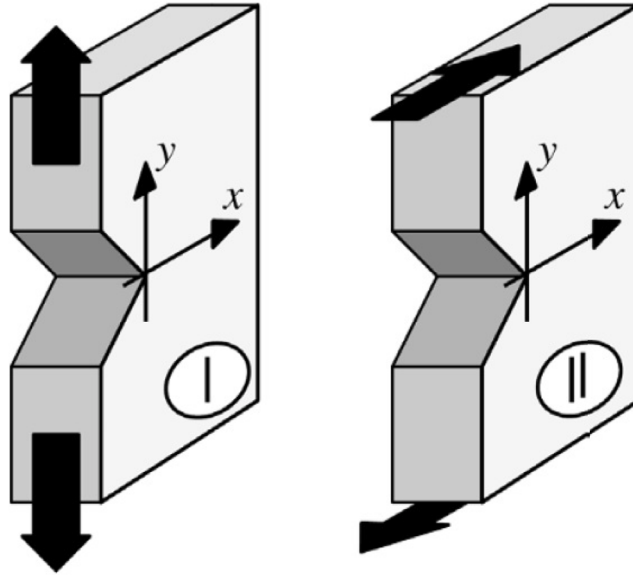


Fig. 2. An elastic plate having a notch in the form of a wedge defined by $0 \leq r \leq R, -\gamma \leq \theta \leq \gamma$ where $r = \sqrt{x^2 + y^2}$ and $\gamma = \tan^{-1} \frac{y}{x}$. The figure shows in plane loading in mode I or mode II.

$$\sigma_{\theta\theta}(r, \theta) = (\alpha + 1)(\alpha + 2)r^\alpha f(\theta) \tag{9}$$

$$\sigma_{r\theta}(r, \theta) = -(1 + \alpha)r^\alpha f'(\theta) \tag{10}$$

The compatibility equation in polar coordinates reads

$$\begin{aligned} \frac{\partial^2 \varepsilon_{\theta\theta}}{\partial r^2} + \frac{1}{r^2} \frac{\partial^2 \varepsilon_{rr}}{\partial \theta^2} + \frac{2}{r} \frac{\partial \varepsilon_{\theta\theta}}{\partial r} - \frac{1}{r} \frac{\partial \varepsilon_r}{\partial r} \\ = \frac{2}{r} \frac{\partial^2 \varepsilon_{r\theta}}{\partial r \partial \theta} + \frac{2}{r^2} \frac{\partial \varepsilon_{r\theta}}{\partial \theta} \end{aligned} \tag{11}$$

and the constitutive equations assuming a varying modulus, but constant Poisson's ratio

$$E(r, \theta) \varepsilon_{rr}(r, \theta) = \sigma_{rr}(r, \theta) - \nu \sigma_{\theta\theta}(r, \theta) \tag{12}$$

$$E(r, \theta) \varepsilon_{\theta\theta}(r, \theta) = \sigma_{\theta\theta}(r, \theta) - \nu \sigma_{rr}(r, \theta) \tag{13}$$

$$E(r, \theta) \varepsilon_{r\theta}(r, \theta) = (1 + \nu) \sigma_{r\theta}(r, \theta) \tag{14}$$

For constant E the compatibility equation turns out not to depend on Poisson's ratio (see Barber, 2002, 11.2)

$$\alpha^2 (\alpha + 2)^2 f(\theta) + (\alpha^2 + (\alpha + 2)^2) f''(\theta) + f^{IV}(\theta) = 0$$

Assuming a solution with a power law elastic modulus in the radial direction

$$E = E_0 r^\beta \tag{15}$$

the Airy function approach leads to a fourth order ODE characteristic equation

$$\begin{aligned} (2 + \alpha)(\alpha - \beta)(\alpha(2 + \alpha - \beta) + \beta(\nu - 1)) f(\theta) + \\ + (4 + 2\alpha(2 + \alpha - \beta) - \beta - \beta(1 + \beta)\nu) f''(\theta) \\ + f^{IV}(\theta) = 0 \end{aligned} \tag{16}$$

which depends on Poisson's ratio, contrary to the homogeneous case. Generally the roots of the associated polynomial are complex and conjugate either in the form

$$x_{1,2} = \pm ia_1, \quad x_{3,4} = \pm ia_2 \tag{17}$$

or in the form

$$x_{1,2} = b_1 \pm ia_1, \quad x_{3,4} = b_2 \pm ia_2 \tag{18}$$

where in this second case $b_2 = -b_1$ and $a_1 = a_2 = a$.

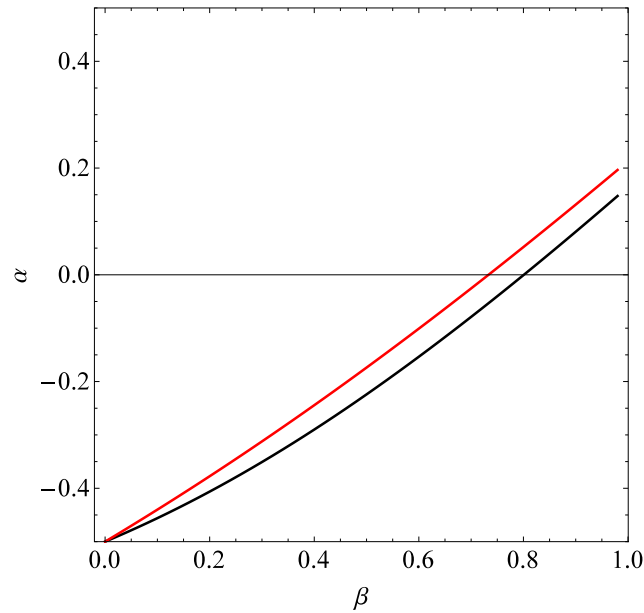


Fig. 3. The eigenvalues of possible power law exponent α in stresses $\sigma \sim r^\alpha$ with a modulus varying as $E \sim r^\beta$ for a crack geometry ($\gamma = \pi$).

The general solution reads

$$f(\theta) = A_1 \exp(b_1\theta) \cos(a_1\theta) + A_2 \exp(b_1\theta) \sin(a_1\theta) + A_3 \exp(-b_1\theta) \cos(a_2\theta) + A_4 \exp(-b_1\theta) \sin(a_2\theta) \tag{19}$$

from which we can extract the various stress component. Notice that when the roots are of the first type (17) we do not have exponential terms, but the 4 solutions are independent because the imaginary parts of the roots are different. Vice versa, when the roots are of the second type (18) we have exponential terms, and the trigonometric terms are the same, but the exponential terms look different, so the solutions are still independent, and no degenerate cases are found.

In a wedge with opening angle $\theta = \pm\gamma$ we need to impose the free traction conditions $\sigma_{\theta\theta}(\pm\gamma) = 0$ and $\sigma_{r\theta}(\pm\gamma) = 0$. This leads to a system of four equations on the factors A_i which has a non-trivial solution only for null determinant. Hence, this gives a non-linear equation which has various solutions in terms of α .

Notice that the strain energy in a region near the root apex given by the product of stresses σ_{ij} and strains ϵ_{ij}

$$U_R = \frac{1}{2} \int_{-\gamma}^{\gamma} \int_0^R \sigma_{ij} \epsilon_{ij} r dr d\theta \sim \int_0^R r^{2\alpha-\beta+1} dr \tag{20}$$

is bounded for a finite radius R (and hence the singularity is physically acceptable) if

$$\alpha > \frac{\beta - 2}{2} \tag{21}$$

which in the homogeneous case $\beta = 0$ simply gives $\alpha > -1$. The author is considering only stresses due to remote loading, so $\sigma \sim r^{-1}$ (concentrated force) and $\sigma \sim r^{-2}$ (concentrated moment) cases are excluded even if they are energetically ok, like for sufficiently negative β . Since in the present MS we are describing solutions due to remote loading, we exclude strong singularities found in $\alpha = \frac{\beta-2}{2}$, similar to the homogeneous case $\alpha = -1$ described in Barber (2002), par.11.2.1).

3. Results

The eigensolutions for the crack case ($\gamma = \pi$) are shown in Fig. 3, assuming a Poisson’s ratio of $\nu = 0.3$ (other values show a weak effect on the singularities). For $\beta > 0$, the two coincident eigenvalues of LEFM (Linear Elastic Fracture Mechanics) corresponding to $\alpha = -0.5$ become distinct and give separate singularities corresponding to symmetric and antisymmetric modes where the symmetric mode is dominant in the inhomogeneous case. For the equivalent case for notch geometry ($\gamma = 3\pi/4$) we obtain Fig. 4, while the discrete eigenvalues change from those well known of the homogeneous Williams case (weaker than the crack case) to the inhomogeneous even weaker case.

To verify the results we conduct a full FEM investigations in ANSYS. A first area is created near the notch apex with unit radius, and then 30 slices are created from radius 1.4^i to 1.4^{i+1} with θ from 0 to 135° (we take advantage of symmetry). The power law elastic modulus is assigned in every slice using the mean radius of the slice and Poisson’s ratio equal to 0.3. A total of about

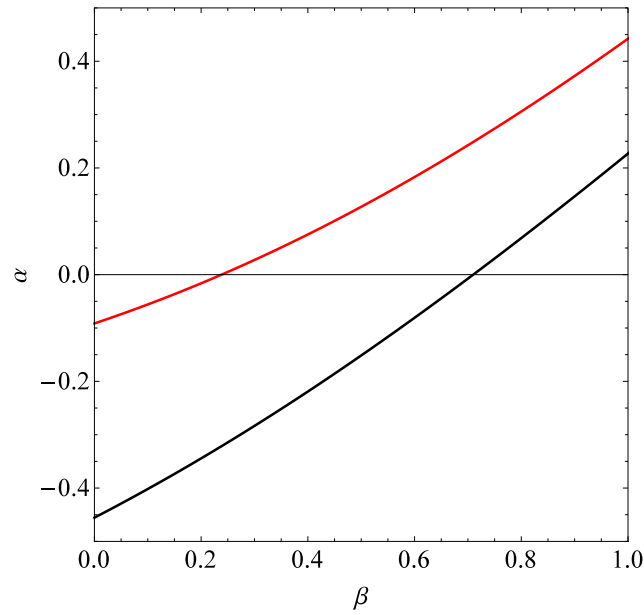


Fig. 4. The eigenvalues α in stresses as in Fig. 3 but for a notch geometry ($\gamma = 3\pi/4$).

16 000 nodes and 5200 elements are created. The line at $y = 0$ is constrained in the u_y direction and one point in particular is also constrained in the u_x direction to avoid rigid body motion.

The FEM model is therefore a wedge defined by $0 \leq r \leq R$, $-\gamma \leq \theta \leq \gamma$ where $\gamma = 3/4\pi$ and is loaded by a radial pressure varying linearly between 0 at $\theta = 0$ and $\sigma_{rr} = \sigma_a$ at $\theta = \pm 3/4\pi$ on the boundary $r = R$ (symmetrical loading). This type of loading is rather arbitrary, but is sufficient for our purpose of being representative. Along the symmetry line $\theta = 0$ we obtain the results of Fig. 5 for the hoop stresses $\sigma_{\theta\theta}$, reported divided by the applied maximum radial stress, and in absolute value to make it evident also the region where they become compressive due to some bending effect. The purple smooth line is the homogeneous case results, which shows the classical singularity of the Williams solution. Increasing the inhomogeneity with $\beta = 0.5, 0.7, 1, 2$ we obtain results indicated by blue, green, red and black curves which appear zig-zagging because the notch is discretized in 30 sectors and in each sector the elastic modulus is necessarily constant by construction. Hence, the zig-zag is obtained from alternating of the homogeneous eigenvalue (as it can be seen from the parallel purple line), and an higher order one, resulting in a curve which “globally” has the slope predicted by the dominant eigenvalue presented in Fig. 4. In particular, notice that the stress becomes non singular for $\beta = 0.7$ (green line) as expected from Fig. 4.

4. Discussion

We have found that the dominant root of the stress field is for graded material a distinct dominant eigenvalue

$$\alpha = \alpha(\beta) \quad (22)$$

which means that at any particular radius from the notch tip we have $\sigma(r) = \sigma_0 r^{\alpha(\beta)}$ while $E(r) = E_0 r^\beta$: using now Eq. (3)

$$\sigma_{allow}(r) = C E^{\delta/p} = C E_0^{\delta/p} r^{\beta\delta/p} \quad (23)$$

and hence

$$\sigma(r) / \sigma_{allow}(r) = \frac{\sigma_0 r^{\alpha(\beta)}}{C E_0^{\delta/p} r^{\beta\delta/p}} = C_1 r^{\alpha(\beta) - \beta\delta/p} \quad (24)$$

where C_1 is a constant. Hence we can keep $\sigma / \sigma_{allow} < 1$ when approaching the notch apex if

$$\alpha(\beta) > \beta\delta/p \quad (25)$$

For simplicity, let us approximate with a linear law the case of $\gamma = 3/4$ and the dominant eigenvalue is found as $\alpha(\beta) = -0.47 + 1.43\beta/2$. Hence, cancelling the singularity involves $\beta > 0.66$ but considering the more refined condition ((25)) gives the shaded regions plotted in Fig. 6. In particular, there are two regions, one to the left of $\delta/p = 0.75$ where “optimal” solution involve *non singular* stresses and β becomes unbounded near $\delta/p = 0.75$, and this region is probably more practical as we have discussed in the introduction. However, there is another region of possible “optimal” solution with singular stresses when the strength increases fast enough with density and it is convenient in this case to have an higher modulus near the notch apex.

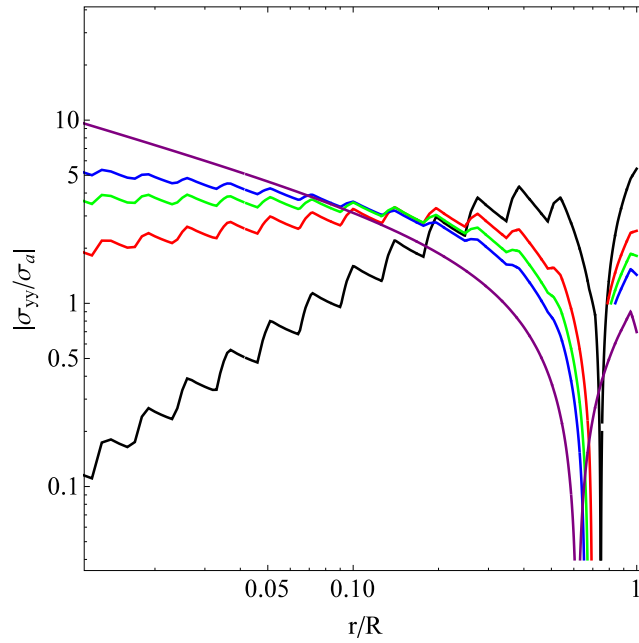


Fig. 5. The hoop stress σ_{yy} along the notch bisector $\theta = 0$ for $\gamma = 3\pi/4$ and various level of power law elastic modulus $E = E_0 r^\beta$. Homogeneous case ($\beta = 0$) is purple smooth line, while $\beta = 0.5, 0.7, 1.2$ are indicated as blue, green, red and black curves which appear zig-zagging because the notch is discretized in 30 sectors and in each sector the elastic modulus is constant.

Specifically, considering Eqs. (1)–(3), $\rho \sim r^{\beta/p}$ and hence $\beta < 0$ implies infinite density at the origin, while $\beta > 0$ implies zero density at the origin. Hence, the ‘singular stress’ optimal region in Fig. 6 corresponds to a case where the power law assumption leads to an infinite allowable stress at the origin, and also infinite density. Also the zero density limit ‘non-singular stress’ optimal region in Fig. 6 is a limit case. In both cases, we can imagine there is a finite sector surrounding the origin of high (or low) but bounded and constant density (or modulus and strength): in this very small region, the classical singularity holds, but in the spirit of all asymptotic solutions, this is however a region to be disregarded if it becomes as small as possible in the manufacturing technique or in the actual physical realization of the notch. Consider additionally that a small but finite rounded corner will be probably be present, as in any notch problem, but this does not preclude the validity of the ideally sharp notch case as in all the entire one hundred years of development of Linear Elastic Fracture Mechanics, from Griffith (1921) on.

In a very interesting recent paper, Liu et al. (2023) have demonstrated experimentally what they call a “crack tip softening (CTS) concept” to simultaneously improve the toughness and threshold of a single polymeric network. By applying light at the crack tip of a sample so that the elastic modulus degrade, fracture toughness and fatigue threshold have been enhanced by about four times. We see that this softening of the elastic modulus is indeed a primitive version of our proposed methodology of grading the elastic modulus, and hence the experimental results of Liu et al. (2023) are highly appropriate here. Liu et al. (2023) also compare their CTS concept with other alternative techniques to improve toughness and fatigue threshold in soft materials, and find their technique competitive. There is therefore hope that with more refinement as suggested in the present paper, even higher increase of strength (in the general sense) are possible.

In another interesting recent paper, Da (2024) has shown that structural design against brittle fracture with topology optimization, which is normally done with the view of optimizing stiffness, can also be done to increase toughness, including in architected materials. Toughness and extreme load-bearing capacity can be improved at the same time. The fact that perforated architecture outperforms homogeneous structures in both toughness and peak load is an indication that, as in our paper, grading density can lead to entirely new strategies for optimal design.

Finally, we remark that our methodology effectively makes a cracked or a notched structure size-scale independent: this comes to a surprise as even Galileo had postulated a certain size effect in his concepts of strength in 1638 (see Galilei, 1638; Salençon, 2006). All materials exhibit size effects in the presence of notches and cracks (see Bažant, 1997; Bazant, 2005), and here we have obtained for the first time the cancelling of such size effect, so that design of a notched structure with the grading suggested can return to more classical strength criteria.

5. Conclusions and outlook

We have discussed how to remove the effect of a sharp V notch by using graded materials with an elastic modulus varying as a power law of the distance from the notch tip. We have shown that with a modulus which increases sufficiently fast away from the

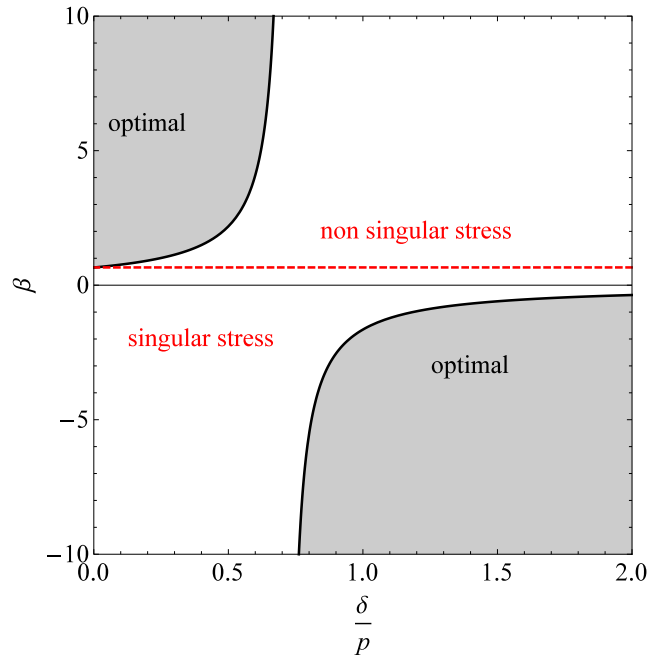


Fig. 6. The range of “optimal” power law β of the elastic modulus variation as a function of the strength-modulus exponent ratio δ/p for a sharp notch with $\gamma = 3/4\pi$ shows that “removing” the sharp notch effect requires not cancelling the singularity but a value of β satisfying the inequality (25).

notch tip, we can cancel the stress singularity. However, since this involves effectively in the limit a zero modulus at the notch tip, it makes sense to consider also a strength which depends as a power law of the density, and therefore of the distance from the notch tip. The latter more complete analysis shows that depending on the strength-modulus exponent ratio δ/p of the material, i.e. how the strength increase with density with respect to the modulus increase, and the notch angle, there are two regions of “optimal” design. The most likely optimal design is that involving an elastic modulus increasing with distance.

While for homogeneous material the case of sharp notch is relatively well understood, for inhomogeneous material, certainly experimental investigation would be beneficial, which is outside the scope of the present paper.

The present methodology paves the way for a more general strategy in the presence of elastic singularities (Sinclair, 2004), like for example in contact problems (Kim et al., 2014; Hills and Dini, 2006; Barber, 2018, Chap.10, Hills and Dini, 2006) where the degree of the singular stress field depends not only on geometry but also on friction coefficient. The application is therefore very wide, involving joint attachments, biomedical field and many machine components not necessarily having an atomically sharp notch, which is clearly an idealization as in fracture mechanics is the atomically sharp crack. We remark that our methodology effectively makes a cracked or a notched structure size-scale independent.

Statement of novelty

To the best of our knowledge no existing work (either submitted or already published, including our own) has a significant overlap with our submission.

CRediT authorship contribution statement

M. Ciavarella: Writing – review & editing, Writing – original draft, Visualization, Validation, Software, Methodology, Investigation, Formal analysis, Data curation, Conceptualization.

Declaration of competing interest

The authors declare that they have no known competing financial interests or personal relationships that could have appeared to influence the work reported in this paper.

Data availability

No data was used for the research described in the article.

Acknowledgements

MC acknowledges support from the Italian Ministry of Education, University and Research (MIUR) under the program “Departments of Excellence” (L.232/2016).

References

- Abdalla, H.M.A., Casagrande, D., De Bona, F., 2023. Analysis of stress concentration in functionally graded plates with linearly increasing Young's modulus. *Materials* 16 (21), 6882.
- Ashby, M.F., 1991. Overview no. 92: Materials and shape. *Acta Metall. Mater.* 39 (6), 1025–1039.
- Barber, J.R., 2002. *Elasticity*. Kluwer academic publishers, Dordrecht.
- Barber, J.R., 2018. *Contact Mechanics*. Springer International Publishing, Berlin.
- Bauer, J., Guell Izard, A., Zhang, Y., Baldacchini, T., Valdevit, L., 2019. Programmable mechanical properties of two-photon polymerized materials: from nanowires to bulk. *Adv. Mater. Technol.* 4 (9), 1900146.
- Bazant, Z.P., 1997. Scaling of quasibrittle fracture: Asymptotic analysis. *Int. J. Fract.* 83, 19–40.
- Bazant, Z.P., 2005. *Scaling of Structural Strength*. Elsevier, Oxford, UK.
- Bendsoe, M.P., Sigmund, O., 1999. Material interpolation schemes in topology optimization (PDF). *Arch. Appl. Mech.* 69 (9–10), 635–654.
- Broek, D., 2012. *The Practical Use of Fracture Mechanics*. Springer Science & Business Media.
- Carpinteri, A., Cornetti, P., Pugno, N., Sapora, A., Taylor, D., 2008. A finite fracture mechanics approach to structures with sharp V-notches. *Eng. Fract. Mech.* 75 (7), 1736–1752.
- Carpinteri, A., Paggi, M., 2005. On the asymptotic stress field in angularly nonhomogeneous materials. *Int. J. Fracture* 135, 267–283.
- Currey, J.D., 1988. The effect of porosity and mineral content on the Young's modulus of elasticity of compact bone. *J. Biomech.* 21 (2), 131–139.
- Da, D., 2024. Structural design against Brittle fracture: Optimizing energy release rate and experiment. *Comput. Methods Appl. Mech. Engrg.* 425, 116935.
- Galilei, G., 1638. *Discorsi E Dimostrazioni Matematiche Intorno a Due Nuove Scienze*. Elsevirii, Leyden.
- Gdoutos, E.E., 2020. *Fracture Mechanics: An Introduction*, Vol. 263, Springer Nature.
- Gibson, L.J., 1989. Modelling the mechanical behavior of cellular materials. *Mater. Sci. Eng. A* 110, 1–36.
- Gibson, L.J., Ashby, M.F., 1997. *Cellular Solids: Structure and Properties*, 2nd Ed. Cambridge University Press, Cambridge.
- Gómez, F.J., Elices, M., 2003. A fracture criterion for sharp V-notched samples. *Int. J. Fract.* 123, 163–175.
- Götzen, N., Cross, A.R., Ifju, P.G., Rapoff, A.J., 2003. Understanding stress concentration about a nutrient foramen. *J. Biomech.* 36 (10), 1511–1521.
- Griffith, A.A., 1921. VI. The phenomena of rupture and flow in solids. *Philos. Trans. R. Soc. London Ser. A* 221 (582–593), 163–198.
- Hills, D.A., Dini, D., 2006. A new method for the quantification of nucleation of fretting fatigue cracks using asymptotic contact solutions. *Tribol. Int.* 39 (10), 1114–1122.
- Huang, J., Venkataraman, S., Rapoff, A.J., Haftka, R.T., 2003. Optimization of axisymmetric elastic modulus distributions around a hole for increased strength. *Struct. Multidiscip. Optim.* 25, 225–236.
- Kim, H.K., Hills, D.A., Paynter, R.J., 2014. Asymptotic analysis of an adhered complete contact between elastically dissimilar materials. *J. Strain Anal. Eng. Des.* 49 (8), 607–617.
- Kossa, A., Hensel, R., McMeeking, R.M., 2023. Adhesion of a cylindrical punch with elastic properties that vary radially. *Mech. Res. Commun.* 130, 104123.
- Kubair, D.V., Bhanu-Chandar, B., 2008. Stress concentration factor due to a circular hole in functionally graded panels under uniaxial tension. *Int. J. Mech. Sci.* 50 (4), 732–742.
- Kumar, P., Sharma, S.K., Singh, R.K.R., 2023. Recent trends and future outlooks in manufacturing methods and applications of FGM: A comprehensive review. *Mater. Manuf. Process.* 38 (9), 1033–1067.
- Lazzarin, P., Campagnolo, A., Berto, F., 2014. A comparison among some recent energy-and stress-based criteria for the fracture assessment of sharp V-notched components under mode I loading. *Theor. Appl. Fract. Mech.* 71, 21–30.
- Lazzarin, P., Zambardi, R., 2001. A finite-volume-energy based approach to predict the static and fatigue behavior of components with sharp V-shaped notches. *Int. J. Fracture* 112, 275–298.
- Li, W., Han, B., 2018. Research and application of functionally gradient materials. In: *IOP Conference Series: Materials Science and Engineering*, vol. 394, IOP Publishing, 022065.
- Liu, Y.X., Thomopoulos, S., Birman, V., Li, J.S., Genin, G.M., 2012. Bi-material attachment through a compliant interfacial system at the tendon-to-bone insertion site. *Mech. Mater.* 44, 83–92.
- Liu, B., Yin, T., Zhu, J., Zhao, D., Yu, H., Qu, S., Yang, W., 2023. Tough and fatigue-resistant polymer networks by crack tip softening. *Proc. Natl. Acad. Sci.* 120 (6), e2217781120.
- Martin, R.B., 1991. Determinants of the mechanical properties of bones. *J. Biomech.* 24, 79–88.
- Meneghetti, G., Lazzarin, P., 2007. Significance of the elastic peak stress evaluated by FE analyses at the point of singularity of sharp V-notched components. *Fatigue Fract. Eng. Mater. Struct.* 30 (2), 95–106.
- Mohammadi, M., Dryden, J.R., Jiang, L., 2011. Stress concentration around a hole in a radially inhomogeneous plate. *Int. J. Solids Struct.* 48 (3–4), 483–491.
- Salençon, J., 2006. Revisiting Galileo's insight in structural mechanics. In: *Conference At the Department of Structural Mechanics*. Budapest University of Technology and Economics, <https://cityu-ias-www-upload.s3.amazonaws.com/migrate/works/prof-jean-salencon/167.pdf>.
- Schumacher, C., Bickel, B., Rys, J., Marschner, S., Daraio, C., Gross, M., 2015. Microstructures to control elasticity in 3D printing. *ACM Trans. Graph. (Tog)* 34 (4), 1–13.
- Seweryn, A., 1994. Brittle fracture criterion for structures with sharp notches. *Eng. Fract. Mech.* 47 (5), 673–681.
- Shi, P.P., 2015. Stress field of a radially functionally graded panel with a circular elastic inclusion under static anti-plane shear loading. *J. Mech. Sci. Technol.* 29, 1163–1173.
- Sinclair, G.B., 2004. Stress singularities in classical elasticity—II: Asymptotic identification. *Appl. Mech. Rev.* 57 (5), 385–439.
- Song, T., Jiang, B., Li, Y., Ji, Z., Zhou, H., Jiang, D., et al., 2021. Self-healing materials: A review of recent developments. *ES Mater. Manuf.* 14, 1–19.
- Suresh, S., Olsson, M., Giannakopoulos, A.E., Padture, N.P., Jitcharoen, J., 1999. Engineering the resistance to sliding-contact damage through controlled gradients in elastic properties at contact surfaces. *Acta Mater.* 47 (14), 3915–3926.
- Zhang, B., Jaiswal, P., Rai, R., Nelaturi, S., 2018. Additive manufacturing of functionally graded material objects: A review. *J. Comput. Inf. Sci. Eng.* 18 (4), 041002.